DONG THAP UNIVERSITY JOURNAL OF SCIENCE
Tạp chí Khoa học Đại học Đồng Tháp
Natural Sciences Issue
ISSN 0866-7675 | e-ISSN 2815-567X

DOI: https://doi.org/10.52714/dthu.ns.2177.1830

INTERACTION MECHANISM OF ENSITRELVIR WITH SARS-COV-2 MAIN PROTEASE AND ITS VARIANTS REVEALED BY MOLECULAR DYNAMICS SIMULATION

Huynh Thi Ngoc Thanh[1], Kieu Nhat Ha[2], and Kieu Minh Nhan[3*]

[1]Faculty of Agriculture, Natural Resources and Environment, Dong Thap University, Cao Lanh 870000, Vietnam

[2]Postgraduate student, Dong Thap University, Vietnam

[3]Office of Facilities and Project Management, Dong Thap University, Cao Lanh 870000, Vietnam

[*]Corresponding author: kmnhan@dthu.edu.vn

Article history

Received: 19/02/2025; Received in revised form: 15/4/2025; Accepted: 24/4/2025

Abstract

SARS-CoV-2 continues to evolve, leading to new variants that may diminish the effectiveness of current treatments. It has undergone genetic mutations, including Alpha (B.1.1.7), Beta (B.1.351), Gamma (P.1), Delta (B.1.617.2), and Omicron (B.1.1.529). The main protease (Mpro) is a key target for antiviral drug development, with various inhibitors currently being investigated as potential COVID-19 treatments. The results of docking and SMD analyses revealed that the binding energy, non-equilibrium work, and rupture force of Ensitrelvir exhibit strong interactions with Mpro, particularly in the K90R mutation, where the non-equilibrium work is 158.8 ± 17.7 kcal.mol^{-1}. This finding aligns well with experimental data, as indicated by the IC_{50} value, showing a correlation coefficient ($R \approx -0.9$). Additionally, the docking results indicated that non-bonded interactions play a crucial role in Ensitrelvir's inhibition of SARS-CoV-2.

Keywords: *Docking method, Ensitrelvir, Mpro, SARS-CoV-2, SMD method.*

Cite: Huynh, T. N. T., Kieu, N. H., & Kieu, M. N. (2026). Interaction mechanism of Ensitrelvir with SARS-CoV-2 main protease and its variants revealed by molecular dynamics simulation. *Dong Thap University Journal of Science, 15*(5), 20-31. https://doi.org/10.52714/dthu.ns.2177.1830

HIỂU RÕ CƠ CHẾ TƯƠNG TÁC CỦA ENSITRELVIR VỚI MAIN PROTEASE CỦA SARS-COV-2 VÀ CÁC BIẾN THỂ BẰNG MÔ PHỎNG ĐỘNG LỰC PHÂN TỬ

Huỳnh Thị Ngọc Thanh[1], Kiều Nhật Hạ[2] và Kiều Minh Nhân[3*]

[1]Khoa Nông nghiệp, Tài nguyên và Môi trường, Trường Đại học Đồng Tháp, Việt Nam

[2]Học viên cao học, Trường Đại học Đồng Tháp, Việt Nam

[3]Phòng Thiết bị và Xây dựng Cơ bản, Đại học Đồng Tháp, Việt nam

[*]Tác giả liên hệ, Email: kmnhan@dthu.edu.vn

Lịch sử bài báo

Ngày nhận: 19/02/2025; Ngày nhận chỉnh sửa: 15/4/2025; Ngày duyệt đăng: 24/4/2025

Tóm tắt

SARS-CoV-2 tiếp tục tiến hóa, dẫn đến xuất hiện nhiều biến thể mới có thể làm giảm hiệu quả của các phương pháp điều trị hiện tại. Virus SARS-CoV-2 đã trải qua các đột biến di truyền, bao gồm Alpha (B.1.1.7), Beta (B.1.351), Gamma (P.1), Delta (B.1.617.2) và Omicron (B.1.1.529). Main protease (Mpro) là một thụ thể quan trọng trong việc phát triển thuốc kháng virus SARS-CoV-2, với các chất ức chế đang được nghiên cứu như những liệu pháp tiềm năng cho COVID-19. Phân tích kết quả docking và SMD cho thấy năng lượng liên kết (ΔE_{bind}), công không cân bằng (W_{pull}) và lực phá vỡ (F_{max}) của Ensitrelvir có tương tác mạnh với Mpro, đặc biệt là trong đột biến K90R, với công không cân bằng đạt 158.8 ± 17.7 kcal.mol^{-1}. Kết quả này hoàn toàn phù hợp với dữ liệu thực nghiệm thông qua giá trị IC_{50}, thể hiện hệ số tương quan ($R \approx -0.9$). Thêm vào đó, kết quả docking còn chỉ ra rằng các tương tác không liên kết đóng vai trò quan trọng trong cơ chế ức chế SARS-CoV-2 của Ensitrelvir.

Từ khóa: *Ensitrelvir, Mpro, Phương pháp docking, Phương pháp SMD, SARS-CoV-2.*

1. Introduction

As of February 2, 2025, the global SARS-CoV-2 situation has been mostly under control due to extensive vaccination efforts and effective public health measures. However, the virus continues to evolve, resulting in new variants that may reduce the effectiveness of current treatments (Davies et al., 2021; Faria et al., 2021). SARS-CoV-2 is a positive-sense single-stranded RNA virus that is transmissible among humans. SARS-CoV-2 has undergone genetic mutations, leading to changes in the virus's structure or behavior. These variants can affect the transmission rate, disease severity, or the effectiveness of treatments and vaccines (Walensky et al., 2021). The World Health Organization (WHO) has declared five variants of concern (VOCs): Alpha (B.1.1.7), Beta (B.1.351), Gamma (P.1), Delta (B.1.617.2), and Omicron (B.1.1.529).

The main protease (Mpro), also known as 3-chymotrypsin-like protease (3CLpro), is a crucial enzyme in the replication cycle of coronaviruses, including SARS-CoV-2. It plays a key role in processing the viral polyproteins into functional proteins necessary for viral replication. Because of its essential role in the viral life cycle (Mondal et al., 2022), 3CLpro has been identified as a potential target for antiviral drug development, with inhibitors being explored as possible treatments for COVID-19 (Owen et al., 2021).

There are thousands of variants of SARS-CoV-2, with each variant carrying mutations in the 3CLpro at different frequencies. These mutations are specific to the Alpha, Beta, Gamma, Lambda, and Omicron variants. Specifically, Alpha (B.1.1.7), Beta (B.1.351), Gamma (P.1) variants exhibit the K90R (M. Lin et al., 2023) substitution, Lambda has the G15S (M. Lin et al., 2023) substitution, and Omicron (B.1.1.529) features the P132H (C. Lin et al., 2023) substitution. It remains uncertain whether these changes in 3CLpro across various SARS-CoV-2 variants will influence the structure of the reaction pocket, potentially affecting the efficacy of current compounds targeting 3CLpro. Several studies have explored the inhibitory potential of Ensitrelvir—a non-covalent, non-peptidic oral inhibitor - against both the wild-type main protease (3CLpro) of SARS-CoV-2 and its variants (Kawashima et al., 2023; C. Lin et al., 2023; M. Lin et al., 2023; Unoh et al., 2022). In particular, the study by Lin et al. conducted quantitative analyses and showed that Ensitrelvir exhibits strong inhibitory activity against the wild-type 3CLpro enzyme as well as the variants carrying the P132H, G15S, and K90R mutations. The corresponding half-maximal inhibitory concentrations (IC_{50}) were determined to be 0.049 μM, 0.050 μM, 0.048 μM, and 0.048 μM, respectively, indicating the promising potential of Ensitrelvir in the treatment of COVID-19 caused by different SARS-CoV-2 variants.

Ensitrelvir is the first orally administered inhibitor of the SARS-CoV-2 main protease (Mpro) that is both non-covalent and non-peptide. It recently received emergency regulatory approval in Japan. In Vietnam, molecular docking and Steered Molecular Dynamics (SMD) have been increasingly applied in antiviral drug screening and molecular mechanism of Ensitrelvir with the SARS-CoV-2 main protease (Huynh et al., 2024), the growing relevance of computational approaches. These studies offer a broader regional context for evaluating our findings (Ngo et al., 2020; Quan et al., 2020).

In this study, the docking and Steered Molecular Dynamics simulations were combined to investigate the interaction mechanism of Ensitrelvir with the SARS-CoV-2 main protease and its variants. The SMD results revealed that Ensitrelvir binds strongly to targets consistent with experimental observations. Specifically, the correlation between non-equilibrium work (W_{pull}) and experimental IC_{50} values was R = -0.8, while the correlation between rupture force (F_{max}) and IC_{50} values was R = -0.9, indicating excellent agreement between simulation and experimental data.

2. Material and methods

2.1. The targets and Ensitrelvir

The molecular structures and binding sites of targets with Ensitrelvir were obtained from the Protein Data Bank (PDB) the following with IDs: 8HBK (WT-Ensitrelvir) (Duan et al., 2023), 8HUX (P132H-Ensitrelvir) (Duan et al., 2023), 8INX (G15S-Ensitrelvir), and 8INY (K90R-Ensitrelvir) (Duan et al., 2023). The 3D structures of these targets are shown in Figure 1, in which the spheres represent the corresponding mutation sites of the variants.

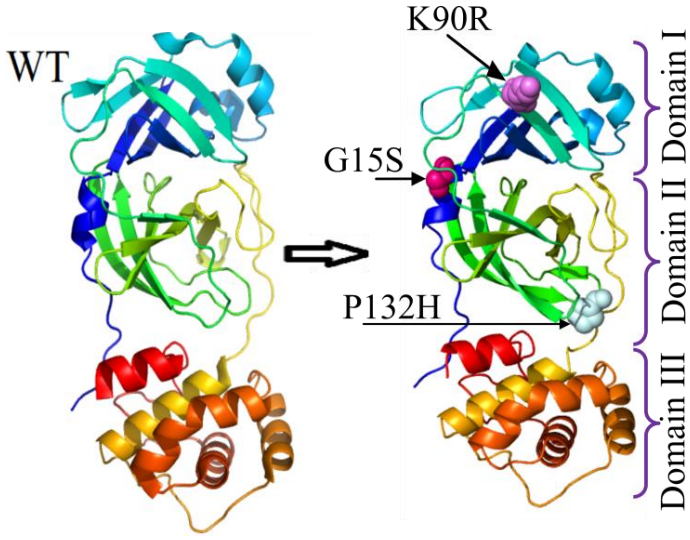

Figure 1. 3D structure of WT (Mpro) and targets with position mutations

Ensitrelvir has synonyms as 2647530-73-0, S-217622, PX665RAA3H… In this paper, ensitrelvir is a compound with CID number 162533924 and chemical formula $C_{22}H_{17}ClF_3N_9O_2$. The molecular structure of Ensitrelvir and its properties are downloaded from the PubChem database (Kim et al., 2025; Sayers et al., 2025). Some properties of Ensitrelvir are shown (Huynh et al., 2024).

2.2. Methods

2.2.1. Docking method

The target molecules will be docked with Ensitrelvir using AutoDock Tool 1.5.4 (Morris et al., 2009; Trott & Olson, 2010). The PDB files: Ensitrelvir, Mpro, K90R, P132H, G15S were converted to PDBQT files by prepare_ligand4.py for ligand, and prepare_receptor4.py for receptor. The ligand docking simulation with the targets was performed by AutoDock Vina version 1.1.2 (Trott & Olson, 2010). To simulate the binding process between the Ensitrelvir and the receptors, we first need to determine the center of the ligand and the size of the box, ensuring that the box size fully encompasses the ligand and the intended binding site. To optimize the selection of the binding site, the exhaustiveness index was set to 400. AutoDock and AutoDock Vina are widely used molecular docking tools validated by numerous studies, with demonstrated accuracy in predicting ligand binding poses (Morris et al., 2009; Trott & Olson, 2010), which are 23,433 and 34,438 citations, respectively.

In AutoDock Vina version 1.1, the dynamics of the ligand's atoms are neglected, and ligand flexibility is approximated during the docking process. The center of the ligand varies for each receptor and is specified in Table 1.

Table 1. The center and size of box

	Center	Box size (Å)
WT	x = -21.75 y = -11.26 z = 2.66	x = 25.00 y = 25.00 z = 25.00
P132H	x = -18.04 y = -12.82 z = 4.39	x = 25.00 y = 25.00 z = 25.00
G15S	x = -21.71 y = -11.22 z = 2.75	x = 25.00 y = 25.00 z = 25.00
K90R	x = -20.71 y = -10.24 z = 2.00	x = 25.00 y = 25.00 z = 25.00

2.2.2. Measures used in data analysis

Non-bonded interactions between the ligand and receptor residues occur when their centers of mass are separated by less than 0.65 nm. A hydrogen bond (HB) is established when the H-A distance is below 0.27 nm, and the angle D-H-A is greater than 135 degrees, the distance between the donor (D) and acceptor (A) is less than 0.35 nm (Thai et al., 2017).

2.2.3. Steered molecular dynamics

The Steered Molecular Dynamics (SMD) method is widely applied to study the mechanical unfolding of biomolecules with 1,253 citations (Israelewitz et al., 2001; Kumar & Li, 2010), and the directional detachment of ligands from receptors (Grubmüller et al., 1996). This approach employs a pulling force along a defined direction to determine the most efficient pathway for ligand dissociation. Specifically, the MSH (Minimal Steric Hindrance) method (Vuong et al., 2015) exerts a constant pulling velocity v on a dummy atom, with the applied force given by $F = k(\Delta z - vt)$, where Δz denotes the displacement of the pulled atom from its initial position. Furthermore, a harmonic potential with a spring constant of 1000 kJ.nm^{-1}.mol^{-1} was enforced on the C-alpha atoms to preserve the structural integrity of the target (Thai et al., 2017).

In this study, the pulling rate is set at 0.005 nm.ps^{-1}, with a pulling constant of 600 kJ.nm^{-1}.mol^{-1}. The pulling force is applied on the center of mass of Ensitrelvir along the z-axis. Within the SMD approach, the maximum force (F_{max}) recorded in the force-extension or non-equilibrium work W_{pull} as an indicator of binding affinity. A greater W_{pull} signifies a stronger interaction between the ligand and its target (Thai et al., 2017). W_{pull} is defined as follows:

$$W_{pull} = \int_0^{x_{max}} \vec{F}.\overrightarrow{dx}$$

$$\approx \sum_1^{N_{step}} \frac{(F_{i+1} + F_i)}{2}(x_{i+1} - x_i), \quad (1)$$

where N_{step} is the total number of steps used in simulation. Thus instead of integral the summation by the trapezoidal rule is used for estimating the non-equilibrium work performed on the system.

All docking and SMD simulations were performed on two Linux-based computer system with the following configurations: (1) OS: Ubuntu 22.04.1 LTS x86_64; Packages: 2025 (dpkg), 13 (snap); CPU: Intel i9-9900K (16) @ 5.000GHz; GPU: NVIDIA GeForce

RTX 2080 Ti; Memory: 2922MiB / 32033MiB. (2) OS: Ubuntu 22.04.5 LTS x86_64; Packages: 2275 (dpkg), 13 (snap); CPU: Intel i9-11900K (16) @ 5.100GHz; GPU: NVIDIA GeForce RTX 1060 6GB; Memory: 1263MiB / 31927MiB.

3. Results and discussion

3.1. Scoring using docking

The docking results of the Ensitrelvir with the Main protease and its mutations: P132H, G15S, K90R, the obtained binding energies were respectively: -9.4 kcal.mol^{-1}, -10 kcal.mol^{-1}, -9.5 kcal.mol^{-1}, and -9.3 kcal.mol^{-1}, which are nearly micromole (μM) of IC_{50} value. The results indicate that the compound Ensitrelvir binds strongly to the Main protease and its mutations. Among them, the P132H mutation has the strongest binding, with the lowest energy level of -10.0 kcal.mol^{-1} for the lowest IC_{50} value respectively. On average, each docking simulation required approximately 5 minutes of computational time per ligand-receptor complex.

Table 2. The binding energies were obtained by docking and calculated using the formula $\Delta G_{exp} = RTln(IC_{50})$

Name	ΔE_{bind} (kcal.mol^{-1})	IC50 (μM) (M. Lin et al., 2023)	ΔG_{exp} (kcal.mol^{-1})
Main protease (8HBK)	-9.4	0.049 ± 0.001	-10.03
P132H (8HUX)	-10.0	0.050 ± 0.001	-10.02
G15S (8INX)	-9.5	0.049 ± 0.002	-10.03
K90R (8INY)	-9.3	0.048 ± 0.001	-10.05

From Figure 2, it showed that Ensitrelvir binds to pocket of the between domain I and domain II for targets. This result is consistent with the experimental results and the binding energies of the system are nearly as expected, as indicated in the Table 2.

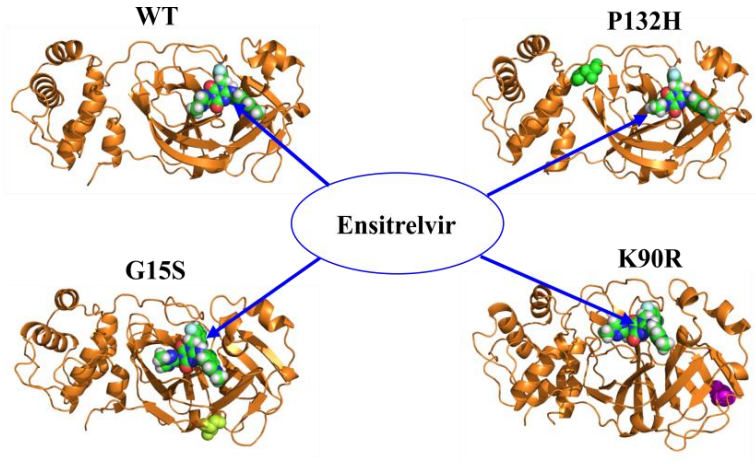

Figure 2. The binding positions of Ensitrelvir with the Main protease of SARS-CoV-2 and its mutations

The experiments have shown that the G15S, K90R, and P132H mutations of SARS-CoV-2 Mpro have very limited effects on the structure and enzymatic properties of Mpro. In fact, the mutated positions 15 and 90 are amino acids located in domain I of Mpro, while the mutated position 132 is an amino acid in domain II. These positions are far from the substrate pocket, which is why the structure of the substrate pocket of Mpro is not affected by these mutations. This also explains why the binding energies of the Ensitrelvir ligand with

the P132H, G15S, and K90R receptors does not differ significantly from that of Mpro (M. Lin et al., 2023).

From the in vitro experimental research conducted by Lin and colleagues (M. Lin et al., 2023), the IC_{50} values of the Ensitrelvir ligand interacting with Mpro and its mutations are presented in Table 2. Using these IC_{50} values, the estimated binding energy variation between Mpro and its mutations with Ensitrelvir can be calculated using the formula ΔG_{exp} = RTln(IC_{50}), where gas constant R = 1.987 x 10^{-3} kcal.mol^{-1}, IC_{50} is measured in mol (M), and T = 300 K.

The ΔG_{exp} values and the binding energy values obtained from the docking method in Table 3 demonstrate a strong consistency. This indicates that Ensitrelvir can effectively inhibit SARS-CoV-2 Mpro and its mutations.

3.2. The binding energy and hydrogen bonding play a minor role

The simulation results show the binding energies of the Ensitrelvir with receptors, including Mpro, G15S, K90R, and P132H, as presented in Table 2. To better, understand the interaction between the Mpro receptor of SARS-CoV-2 and its mutations with the ligand Ensitrelvir. Figure 3 illustrates the types of bonds involved in the complex formation, which includes two main types: hydrogen bonds and Van der Waals interactions (non-bonded contacts). Blue lines represent hydrogen bonds, while red lines represent non-bonded contacts. These diagrams were generated using LigPlot+ version 2.2.8 (Wallace et al., 1995).

The binding energy between Ensitrelvir and the Mpro of SARS-CoV-2 is -9.4 kcal.mol^{-1} (Table 2), with 18 interactions, including 5 hydrogen bonds and 13 non-bonded contacts. The five hydrogen bonds are formed by four amino acids: Glu166, Gly143, Cys145, and Ser144, with Ser144 forming two bonds with the ligand. The amino acids involved in non-bonded interactions between Mpro and Ensitrelvir are Thr26, His163, Phe140, Leu141, Asn142, Thr25, His164, His41, Met165, His172, Ser46, Met49, and Arg188.

For Mpro mutations, the binding energies of Ensitrelvir with P132H, G15S, and K90R are -10 kcal.mol^{-1}, -9.5 kcal.mol^{-1}, and -9.3 kcal.mol^{-1}, respectively, with the total number of amino acids involved in binding being 15, 16, and 17. The number of hydrogen bonds for each mutation is 4, 4, and 6, while the number of non-bonded interactions is 11, 12, and 11, respectively.

The detailed list of amino acids involved in the bonding process is presented in Table 3. Based on Figure 3 and the Table 3 listing the amino acids involved in bond formation during the binding process between Ensitrelvir and the Mpro receptors, as well as its variants, the amino acids that form hydrogen bonds are Glu166, Gly143, Cys145, and Ser144. Notably, in the case of Mpro, the amino acid Ser144, and in the K90R mutation, the amino acid Cys145, each forms two hydrogen bonds with the ligand.

Non-bonded interactions: For the P132H mutation, 11 amino acids participate in forming bonds with the Ensitrelvir ligand, including Thr24, and the remaining amino acids: Thr26, His163, Phe140, Leu141, Asn142, Thr25, His164, His41, Met165, and His172, which are the same amino acids involved in forming bonds between Mpro of SARS-CoV-2 and Ensitrelvir.

For the G15S mutation, 12 amino acids participate in non-bonded interactions with the Ensitrelvir ligand, including Thr26, His163, Phe140, Leu141, Asn142, Thr25, His164, His41, Met165, Met49, Leu27, and Arg188. Notably, except for Leu27, the remaining amino acids are the same as those involved in interactions between Mpro and Ensitrelvir.

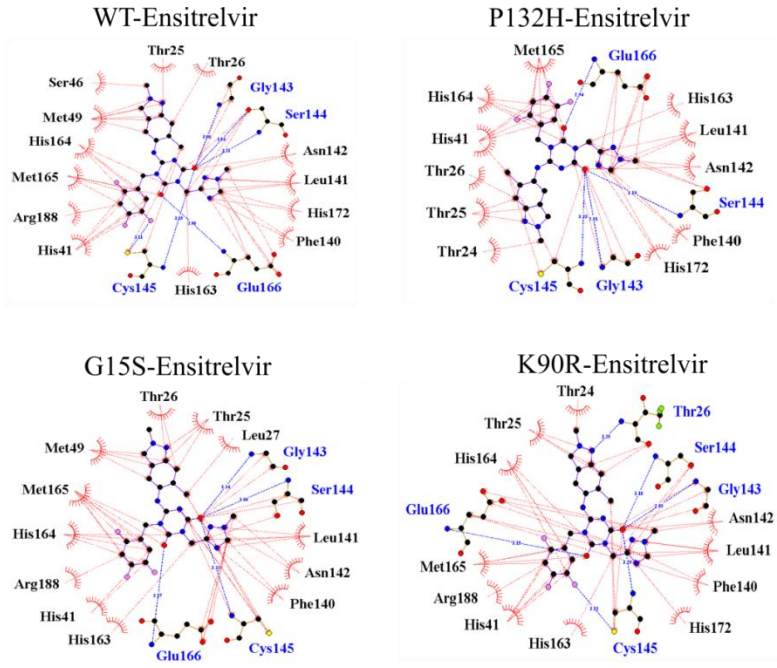

Figure 3. The hydrogen bonds (HBs) are represented in green, while the non-bonded contacts (NBCs) are shown as red lines

For the K90R mutation, 11 amino acids participate in forming non-bonded interactions with the Ensitrelvir drug. Among them, the amino acids that are similar to those in Mpro and form bonds with Ensitrelvir are His163, Phe140, Leu141, Asn142, Thr25, His164, His41, Met165, His172, Arg188, and one amino acid, Thr24, which is also similar to that in the P132H mutation.

Table 3. List of amino acids forming HBs, NBCs between Ensitrelvir and Mpro, and its mutations

Name's Mpro	HBs/ NBCs	Hydrogen bonds	Non bond contacts
Main protease (8HBK)	5/13	Gly143, Ser144 (2), Cys145, Glu166	Thr26, His163, Phe140, Leu141, Asn142, Thr25, His164, His41, Met165, His 172, Ser46, Met49, Arg188,
P132H (8HUX)	4/11	Gly143, Ser144, Cys145, Glu166,	Thr26, His163, Phe140, Leu141, Asn142, Thr25, His164, His41, Met165, His172, Thr24,
G15S (8INX)	4/12	Gly143, Ser144, Cys145, Glu166	Thr26, His163, Phe140, Leu141, Asn142, Thr25, His164, His41, Met165, Met49, **Leu27**, Arg188,
K90R (8INY)	6/11	Thr26, Gly143, Ser144, Cys145 (2), Glu166.	His163, Phe140, Leu141, Asn142, Thr25, His164, His41, Met165, His172, Arg188, Thr24,

This indicates that the number of hydrogen bonds in the complex formed between the Ensitrelvir ligand and the receptors is relatively limited. Meanwhile, non-bonded interactions dominate the binding process, suggesting that Van der Waals interactions play a crucial role in Ensitrelvir's inhibition of SARS-CoV-2.

3.3. The results of SMD

By employing the MSH method, we identified the optimal pulling direction for Ensitrelvir, in which the molecule is positioned in its most favorable docking mode with the receptor. This is showed in Figure 4.

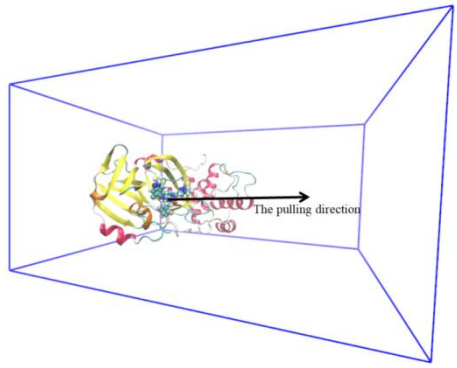

Figure 4. The pulling direction of Ensitrelvir was obtained by MSH (Huynh et al., 2024)

In the docking approach, receptors (targets) are considered rigid; therefore, docking results are primarily used for virtual screening. The SMD method provides binding affinity estimates that are as accurate as the MM-PBSA (molecular mechanics Poisson–Boltzmann surface area) method while being significantly less computationally intensive. However, a limitation of this method is that it predicts only relative binding affinities rather than absolute binding free energies, meaning that ligand binding strength cannot be definitively concluded based on its results alone. In SMD, a higher non-equilibrium work (W_{pull}) or rupture force (F_{max}) indicates stronger binding.

In this study, non-equilibrium work (W_{pull}) or rupture force (F_{max}) were averaged over 15 independent trajectories. Each trajectory was initiated from the same docking configuration but used a different random seed to introduce variability. The length of each SMD simulation was 600 ps, resulting in a total simulation time of 9 ns. SMD has been validated and successfully applied in previous studies for ranking ligand binding affinities (Thai et al., 2017; Vuong et al., 2015).

The Figure 5 is showed force-position profile for Ensitrelvir and targets. To calculate the non-equilibrium work (W_{pull}) for ranking binding affinities, given by Equation (1), the force-time/position curves were used.

As illustrated in Figure 5, the rupture force (F_{max}) manifests at different position scales depending on the specific system under investigation. Despite these variations, the rupture forces (F_{max}) of the Mpro in its wild-type form and the P132H mutant exhibit similar magnitudes. In contrast, the peak forces observed for the G15S and K90R mutants are noticeably higher, with K90R displaying the most pronounced peak among all cases. These findings indicate that Ensitrelvir demonstrates a stronger binding affinity to the G15S and K90R variants compared to the wild type and P132H, which aligns exceptionally well with the experimental data presented in Table 4. Furthermore, this conclusion is supported by the correlation coefficient, which is calculated as R = -0.9 for the rupture force (F_{max}). In a manner similar to the rupture force (F_{max}), the non-equilibrium work (W_{pull}) required to achieve rupture is determined through SMD simulations. The correlation between rupture force (F_{max}) and experimental free energies, as well as between non-equilibrium work (W_{pull}) and experimental free energies, is presented in Figure 6.

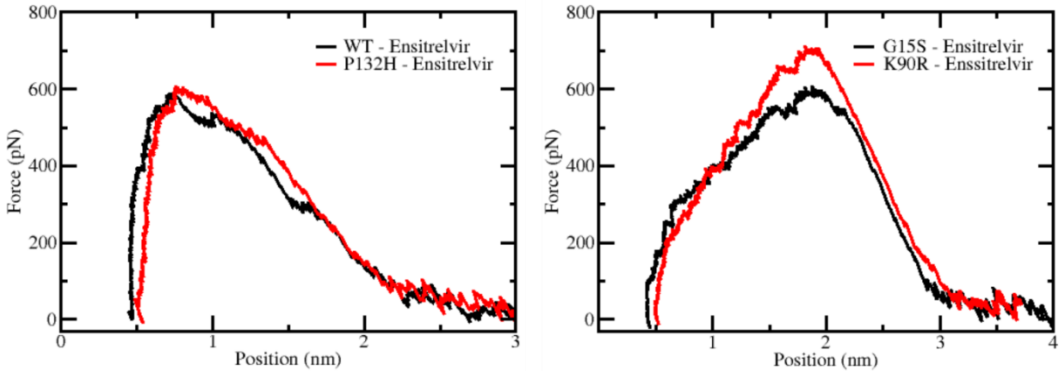

Figure 5. Typical force-position profiles for Ensitrelvir bound to multiple targets

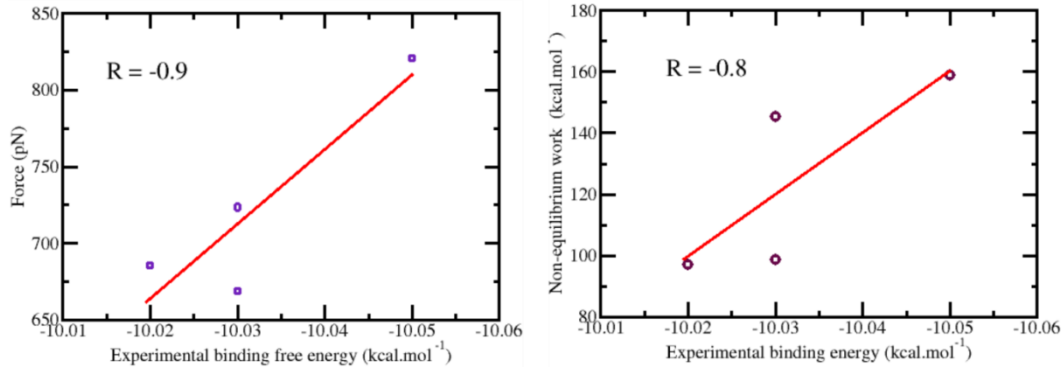

Figure 6. Correlation between rupture force (F_{max})(left), non-equilibrium work (W_{pull}) (right) and experimental free energies.

Table 4. Rupture force (F_{max}), non-equilibrium work (W_{pull}) were obtained by SMD

Name's Mpro	Rupture force (F_{max}) (pN)	Non-equilibrium work (W_{pull}) (kcal.mol^{-1})
Main protease (8HBK)	668.6 ± 44.9	98.7 ± 6.7
P132H (8HUX)	685.1 ± 60.7	96.8 ± 6.3
G15S (8INX)	723.5 ± 91.4	145.2 ± 14.9
K90R (8INY)	820.6 ± 108.6	158.8 ± 17.7

4. Conclusion

Utilizing molecular docking, we evaluated the binding affinities of Ensitrelvir to Mpro (wild type) and its variants. The computed binding affinities are as follows: WT-Ensitrelvir (ΔE_{bind} = -9.4 kcal.mol^{-1}), P132H-Ensitrelvir (ΔE_{bind} = -10.0 kcal.mol^{-1}), G15S-Ensitrelvir (ΔE_{bind} = -9.5 kcal.mol^{-1}), and K90R-Ensitrelvir (ΔE_{bind} = -9.3 kcal.mol^{-1}). The binding energy values correspond to the estimated inhibitory constant in the micromole range. However, the correlation between docking-derived binding energies and experimental IC_{50} values is relatively weak. To further elucidate this discrepancy, we employed SMD simulations to analyze position-dependent force profiles. From these, we extracted the maximum force and non-equilibrium work, which exhibited a strong inverse correlation (R = -0.9) with experimental IC_{50} values. This finding supports the reliability of the SMD approach for assessing binding strength in this system.

Overall, our findings confirm that Ensitrelvir exhibits strong and consistent interactions with both the wild-type Mpro and its key variants. These results align well with

previous simulations (Lin et al., 2023) and support the therapeutic potential of Ensitrelvir in targeting diverse strains of SARS-CoV-2.

Competing Interest: The authors declare no competing financial interest.

Acknowledgements: This research is supported by the project SPD2024.01.08.

References

Davies, N. G., Abbott, S., Barnard, R. C., Jarvis, C. I., Kucharski, A. J., Munday, J. D., Pearson, C. A., Russell, T. W., Tully, D. C., & Washburne, A. D. (2021). Estimated transmissibility and impact of SARS-CoV-2 lineage B. 1.1. 7 in England. *Science, 372*(6538), eabg3055. https://doi.org/10.1126/science.abg3055

Duan, Y., Zhou, H., Liu, X., Iketani, S., Lin, M., Zhang, X., Bian, Q., Wang, H., Sun, H., Hong, S. J., Culbertson, B., Mohri, H., Luck, M. I., Zhu, Y., Liu, X., Lu, Y., Yang, X., Yang, K., Sabo, Y., Chavez, A., Goff, S. P., Rao, Z., Ho, D. D., & Yang, H. (2023). Molecular mechanisms of SARS-CoV-2 resistance to nirmatrelvir. *Nature, 622*(7982), 376-382. https://doi.org/10.1038/s41586-023-06609-0

Faria, N. R., Mellan, T. A., Whittaker, C., Claro, I. M., Candido, D. d. S., Mishra, S., Crispim, M. A., Sales, F. C., Hawryluk, I., & McCrone, J. T. (2021). Genomics and epidemiology of the P. 1 SARS-CoV-2 lineage in Manaus, Brazil. *Science, 372*(6544), 815-821. https://doi.org/10.1126/science.abh2644

Grubmüller, H., Heymann, B., & Tavan, P. (1996). Ligand binding: molecular mechanics calculation of the streptavidin-biotin rupture force. *Science, 271*(5251), 997-999. https://doi.org/10.1126/science.271.5251.997

Huynh, T. N. T., Kieu, M. N., Kieu, N. H., & Nguyen Quoc, T. (2024). Molecular mechanism of Ensitrelvir and its similarity inhibiting SARS-CoV-2 main protease by molecular dynamics simulation. *Tạp chí Khoa học Đại học Đồng Tháp, 13*(5), 37-44. https://doi.org/10.52714/dthu.13.5.2024.1286

Isralewitz, B., Gao, M., & Schulten, K. (2001). Steered molecular dynamics and mechanical functions of proteins. *Current Opinion in Structural Biology, 11*(2), 224-230. https://doi.org/10.1016/S0959-440X(00)00194-9

Kawashima, S., Matsui, Y., Adachi, T., Morikawa, Y., Inoue, K., Takebayashi, S., Nobori, H., Rokushima, M., Tachibana, Y., & Kato, T. (2023). Ensitrelvir is effective against SARS-CoV-2 3CL protease mutants circulating globally. *Biochemical and Biophysical Research Communications, 645*, 132-136. https://doi.org/10.1016/j.bbrc.2023.01.040

Kim, S., Chen, J., Cheng, T., Gindulyte, A., He, J., He, S., Li, Q., Shoemaker, B. A., Thiessen, P. A., Yu, B., Zaslavsky, L., Zhang, J., & Bolton, E. E. (2025). PubChem 2025 update. *Nucleic Acids Res, 53*(D1), D1516-d1525. https://doi.org/10.1093/nar/gkae1059

Kumar, S., & Li, M. S. (2010). Biomolecules under mechanical force. *Physics Reports, 486*(1-2), 1-74. https://doi.org/10.1016/j.physrep.2009.11.001

Lin, C., Jiang, H., Li, W., Zeng, P., Zhou, X., Zhang, J., & Li, J. (2023). Structural basis for the inhibition of coronaviral main proteases by ensitrelvir. *Structure, 31*(9), 1016-1024.e1013. https://doi.org/10.1016/j.str.2023.06.010

Lin, M., Zeng, X., Duan, Y., Yang, Z., Ma, Y., Yang, H., Yang, X., & Liu, X. (2023). Molecular mechanism of ensitrelvir inhibiting SARS-CoV-2 main protease and its variants. *Communications Biology, 6*(1), 694. https://doi.org/10.1038/s42003-023-05071-y

Mondal, S., Chen, Y., Lockbaum, G. J., Sen, S., Chaudhuri, S., Reyes, A. C., Lee, J. M., Kaur, A. N., Sultana, N., & Cameron, M. D. (2022). Dual inhibitors of main protease

(MPro) and Cathepsin L as potent antivirals against SARS-CoV2. *Journal of the American Chemical Society, 144*(46), 21035-21045. https://pubs.acs.org/doi/10.1021/jacs.2c04626

Morris, G. M., Huey, R., Lindstrom, W., Sanner, M. F., Belew, R. K., Goodsell, D. S., & Olson, A. J. (2009). AutoDock4 and AutoDockTools4: Automated docking with selective receptor flexibility. *Journal of Computational Chemistry, 30*(16), 2785-2791. https://doi.org/10.1002/jcc.21256

Ngo, S. T., Quynh Anh Pham, N., Thi Le, L., Pham, D.-H., & Vu, V. V. (2020). Computational determination of potential inhibitors of SARS-CoV-2 main protease. *Journal of Chemical Information and Modeling, 60*(12), 5771-5780. https://pubs.acs.org/doi/10.1021/acs.jcim.0c00491

Owen, D. R., Allerton, C. M., Anderson, A. S., Aschenbrenner, L., Avery, M., Berritt, S., Boras, B., Cardin, R. D., Carlo, A., & Coffman, K. J. (2021). An oral SARS-CoV-2 Mpro inhibitor clinical candidate for the treatment of COVID-19. *Science, 374*(6575), 1586-1593. https://doi.org/10.1126/science.abl4784

Quan, P. M., Toan, T. Q., Tung, N. S., Dan, N. T., Thuy, T. T. T., Cuong, N. M., & Long, P. Q. (2020). Initial study on SARS-CoV-2 main protease inhibition mechanism of some potential drugs using molecular docking simulation. *Vietnam Journal of Science and Technology, 58*(6), 665-675. https://doi.org/10.15625/2525-2518/58/6/14914

Sayers, E. W., Beck, J., Bolton, E. E., Brister, J. R., Chan, J., Connor, R., Feldgarden, M., Fine, A. M., Funk, K., Hoffman, J., Kannan, S., Kelly, C., Klimke, W., Kim, S., Lathrop, S., Marchler-Bauer, A., Murphy, T. D., O'Sullivan, C., Schmieder, E., Skripchenko, Y., Stine, A., Thibaud-Nissen, F., Wang, J., Ye, J., Zellers, E., Schneider, V. A., & Pruitt, K. D. (2025). Database resources of the National Center for Biotechnology Information in 2025. *Nucleic Acids Res, 53*(D1), D20-d29. https://doi.org/10.1093/nar/gkae979

Thai, N. Q., Nguyen, H. L., Linh, H. Q., & Li, M. S. (2017). Protocol for fast screening of multi-target drug candidates: Application to Alzheimer's disease. *Journal of Molecular Graphics and Modelling, 77*, 121-129. https://doi.org/10.1016/j.jmgm.2017.08.002

Trott, O., & Olson, A. J. (2010). AutoDock Vina: improving the speed and accuracy of docking with a new scoring function, efficient optimization, and multithreading. *Journal of Computational Chemistry, 31*(2), 455-461. https://doi.org/10.1002/jcc.21334

Unoh, Y., Uehara, S., Nakahara, K., Nobori, H., Yamatsu, Y., Yamamoto, S., Maruyama, Y., Taoda, Y., Kasamatsu, K., & Suto, T. (2022). Discovery of S-217622, a noncovalent oral SARS-CoV-2 3CL protease inhibitor clinical candidate for treating COVID-19. *Journal of Medicinal Chemistry, 65*(9), 6499-6512. https://doi.org/10.1021/acs.jmedchem.2c00117

Vuong, Q. V., Nguyen, T. T., & Li, M. S. (2015). A new method for navigating optimal direction for pulling ligand from binding pocket: application to ranking binding affinity by steered molecular dynamics. *Journal of Chemical Information and Modeling, 55*(12), 2731-2738. https://pubs.acs.org/doi/abs/10.1021/acs.jcim.5b00386

Walensky, R. P., Walke, H. T., & Fauci, A. S. (2021). SARS-CoV-2 Variants of Concern in the United States—Challenges and Opportunities. *Jama, 325*(11), 1037-1038. https://doi.org/10.1001/jama.2021.2294

Wallace, A. C., Laskowski, R. A., & Thornton, J. M. (1995). LIGPLOT: a program to generate schematic diagrams of protein-ligand interactions. *Protein Eng, 8*(2), 127-134. https://doi.org/10.1093/protein/8.2.127